SICE Journal of Control, Measurement, and System Integration, Vol. 9, No. 5, pp. 216–224, September 2016

Convergence Rate Analysis of Multi-Agent Positive Systems under Formation Control: An Efficient Algorithm by Exploiting Positivity

Yoshio EBIHARA [*], Dimitri PEAUCELLE [**], and Denis ARZELIER [**]

Abstract : This paper is concerned with convergence rate analysis of multi-agent positive systems under formation control. Recently, we have shown that very basic multi-agent systems under formation control can be modeled as interconnected positive systems, and desired formation can be achieved by designing interconnection matrices appropriately. In such formation control, the resulting convergence performance (i.e., convergence rate) varies according to the interconnection matrices and this fact motivates us to develop an efficient algorithm for the analysis of the convergence rate. In this paper, assuming that the dynamics of agents are positive and homogeneous, we conceive such an algorithm by problem decomposition. We show that the decomposition to smaller size problems and drastic reduction of computational burden become possible by making full use of the positivity of the agents.

Key Words : positive systems, formation control, convergence rate analysis.

1. Introduction

A linear time-invariant (LTI) system is said to be positive if its state and output are both nonnegative for any nonnegative initial state and nonnegative input [1],[2]. The theory of positive system is deeply rooted in the theory of nonnegative matrices [3]–[5], and celebrated Perron-Frobenius theorem [5] has played a central role in analysis and synthesis. Recently, positive system theory has gained renewed interest from the viewpoint of convex optimization, and fruitful results have been obtained along this line, see, e.g., [6]–[11]. On the other hand, Valcher and Misra [12] and Ebihara et al. [13]–[16] focus on the study of multi-agent systems assuming that the agents are all positive. From broad perspective, we could say that the information exchanged by agents is often physical quantity being intrinsically nonnegative and this is the motivation to consider multi-agent positive systems. Another motivation is the fact that simple dynamical systems such as integrator and first-order lag and their series/parallel connections are all positive, and these are typical dynamics of moving objects. It is known that large-scale systems constructed from those subsystems exhibit complicated behavior and deserve investigation in the study area of consensus/formation control of multi-agent systems [17]–[19]. Motivated by these facts, we dealt with multi-agent positive systems by modeling such a system as an interconnected system constructed from positive subsystems and a nonnegative interconnection matrix. In particular, in the context of formation control, we showed an efficient method to design a communication scheme (i.e., the interconnection matrix) over the agents to achieve prescribed formation [15],[20]. This result naturally leads us to develop an efficient algorithm to analyze the convergence performance (i.e., convergence rate) by actively using positivity.

Since the multi-agent positive system of interest is LTI, its convergence rate under formation control can be determined by the dominant pole of the corresponding interconnected positive systems. (The dominant pole is often called algebraic connectivity in the study area of multi-agent systems [17].) Even though we can compute the dominant pole by directly computing all of the eigenvalues of the coefficient matrices of the interconnected system, such a straightforward method is computationally demanding especially when the dimension/number of agents becomes larger. In this paper, we therefore propose an efficient algorithm for dominant pole computation assuming that the dynamics of positive agents are homogeneous. We conceive the algorithm by decomposing the original large size problem into small size problems and exploiting the positivity of each agent. It turns out that, under a mild condition that the interconnection matrix has positive eigenvalues, the computation can be streamlined drastically. We illustrate by numerical examples that the proposed algorithm is definitely efficient.

A conference version of the present paper has been published in [21]. In the current paper we totally rewrite this section by citing latest papers published recently. We also include a complete proof of Theorem 2 that plays a very important role in developing the efficient algorithm. The proof relies on strong results on stability and H_∞ norm of (discrete-time) positive systems and clearly illustrate how the positivity of subsystems can be exploited to conceive the efficient algorithm.

Notations:

$\mathbb{R}$ ($\mathbb{C}$): the set of real (complex) numbers.
$\mathbb{D}$: $\mathbb{D} := \{\nu \in \mathbb{C} : |\nu| \le 1\}$.
$\mathbb{R}^n$: the set of real vectors of size n.
$\mathbb{R}^n_+$: the set of nonnegative vectors of size n.
$\mathbb{R}^n_{++}$: the set of strictly positive vectors of size n.

[*] Department of Electrical Engineering, Kyoto University, Kyotodaigaku-Katsura, Nishikyo-ku, Kyoto 615-8510, Japan. He was also with LAAS-CNRS, F-31400 Toulouse, France in 2011.
[**] LAAS-CNRS, Univ. de Toulouse, CNRS, F-31400 Toulouse, France.
E-mail: ebihara@kuee.kyoto-u.ac.jp
(Received May 10, 2016)
(Revised July 22, 2016)

$\mathbb{R}^{n\times m}$: the set of real matrices of size $n \times m$.
$\mathbb{R}_+^{n\times m}$: the set of nonnegative matrices of size $n \times m$.
$\mathbb{H}^n$: the set of Hurwitz stable matrices of size $n \times n$.
$\mathbb{M}^n$: the set of Metzler matrices of size $n \times n$.
$\sigma(A)$: the set of the eigenvalues of $A \in \mathbb{C}^{n\times n}$.
$\kappa(A)$: the largest real part of $\sigma(A)$.
$\kappa_2(A)$: the second largest real part of $\sigma(A)$.
$\rho(A)$: the spectral radius of $A \in \mathbb{C}^{n\times n}$.
$\mathbb{Z}_N$: $\mathbb{Z}_N := \{1, \cdots, N\}$.

Note that a matrix $A \in \mathbb{R}^{n\times n}$ is said to be Metzler if its off-diagonal entries are all nonnegative, i.e., $A_{ij} \geq 0$ $(i \neq j)$.

2. Basics of Interconnected Positive Systems

Consider the linear system described by

$$G : \begin{cases} \dot{x} = Ax + Bw, \\ z = Cx + Dw \end{cases} \tag{1}$$

where $A \in \mathbb{R}^{n\times n}$, $B \in \mathbb{R}^{n\times n_w}$, $C \in \mathbb{R}^{n_z\times n}$, and $D \in \mathbb{R}^{n_z\times n_w}$. The definition and a basic result of positive systems are now reviewed.

Definition 1 [1] The linear system (1) is said to be *positive* if its state and output are both nonnegative for any nonnegative initial state and nonnegative input.

Proposition 1 [1] The system (1) is positive if and only if $A \in \mathbb{M}^n$, $B \in \mathbb{R}_+^{n\times n_w}$, $C \in \mathbb{R}_+^{n_z\times n}$, and $D \in \mathbb{R}_+^{n_z\times n_w}$.

In this paper, we deal with multi-agent systems where the dynamics of each agent, or say, subsystem, is positive. Consider the positive subsystem G_i $(i \in \mathbb{Z}_N)$ given by

$$G_i : \begin{cases} \dot{x}_i = A_i x_i + B_i w_i, \\ z_i = C_i x_i, \end{cases} \quad A_i \in \mathbb{M}^{n_i} \cap \mathbb{H}^{n_i},\ B_i \in \mathbb{R}_+^{n_i\times n_{w_i}},\ C_i \in \mathbb{R}_+^{n_{z_i}\times n_i}. \tag{2}$$

As clearly shown in (2), we assumed that G_i $(i \in \mathbb{Z}_N)$ are all stable. With these positive subsystems, we define positive and stable system $\mathcal{G}$ by $\mathcal{G} := \mathrm{diag}(G_1, \cdots, G_N)$. The state space realization of $\mathcal{G}$ is given by

$$\mathcal{G} : \begin{cases} \dot{\widehat{x}} = \mathcal{A}\widehat{x} + \mathcal{B}\widehat{w}, \\ \widehat{z} = C\widehat{x} \end{cases} \tag{3}$$

where

$$\mathcal{A} := \mathrm{diag}(A_1, \cdots, A_N),\ \mathcal{B} := \mathrm{diag}(B_1, \cdots, B_N),\ C := \mathrm{diag}(C_1, \cdots, C_N), \tag{4}$$

$$\widehat{x} := \begin{bmatrix} x_1 \\ \vdots \\ x_N \end{bmatrix} \in \mathbb{R}^{n_{\widehat{x}}},\ \widehat{w} := \begin{bmatrix} w_1 \\ \vdots \\ w_N \end{bmatrix} \in \mathbb{R}^{n_{\widehat{w}}},\ \widehat{z} := \begin{bmatrix} z_1 \\ \vdots \\ z_N \end{bmatrix} \in \mathbb{R}^{n_{\widehat{z}}},$$

$$n_{\widehat{x}} := \sum_{i=1}^{N} n_i, \qquad n_{\widehat{w}} := \sum_{i=1}^{N} n_{w_i}, \qquad n_{\widehat{z}} := \sum_{i=1}^{N} n_{z_i}.$$

The multi-agent positive system of interest in this paper is nothing but the interconnected system $\mathcal{G} \star \Omega$ defined by $\widehat{w} = \Omega\widehat{z}$, where $\Omega \in \mathbb{R}_+^{n_{\widehat{w}}\times n_{\widehat{z}}}$ is a given interconnection matrix.

3. Formation Control of Multi-Agent Positive Systems

The goal of this paper is to give an efficient method to analyze the convergence rate performance of multi-agent positive systems under formation control. In this section, we review our preceding results on formation control of multi-agent positive systems and show that a practical formation control of moving agents can be cast as a formation control of multi-agent positive systems.

3.1 Basic Results for Formation Control

The next result forms an important basis for the formation control of the interconnected system $\mathcal{G} \star \Omega$ with respect to the output $\widehat{z}$.

Theorem 1 [15],[20] Consider the case where every stable positive subsystem G_i represented by (2) is SISO. Suppose G_i $(i \in \mathbb{Z}_N)$ and given interconnection matrix $\Omega \in \mathbb{R}_+^{N\times N}$ satisfy the following conditions:

(i) (A_i, B_i) is controllable and (A_i, C_i) is observable for all $i \in \mathbb{Z}_N$.
(ii) $G_1(0) = \cdots = G_N(0) =: \gamma(> 0)$ holds for $G_i(s) := C_i(sI - A_i)^{-1}B_i$ $(i \in \mathbb{Z}_N)$.
(iii) $\Omega \in \mathbb{R}_+^{N\times N}$ is irreducible (i.e., the directed graph of Ω, denoted by $\Gamma(\Omega)$, is strongly connected).
(iv) $\Omega v_{\mathrm{obj}} = (1/\gamma)v_{\mathrm{obj}}$ holds for given $v_{\mathrm{obj}} \in \mathbb{R}_{++}^N$.

Then, the output of interconnected system $\mathcal{G} \star \Omega$ satisfies

$$\widehat{z}_\infty = \gamma\alpha(\widehat{x}(0))v_{\mathrm{obj}}, \quad \widehat{z}_\infty := \lim_{t\to\infty}\widehat{z}(t) \tag{5}$$

where

$$\alpha(\widehat{x}(0)) := \xi_{\mathrm{L}}^T\widehat{x}(0)/\xi_{\mathrm{L}}^T\xi_{\mathrm{R}} \in \mathbb{R}, \quad \xi_{\mathrm{R}} = -\mathcal{A}^{-1}\mathcal{B}v_{\mathrm{obj}} \in \mathbb{R}_{++}^{n_{\widehat{x}}},\ \xi_{\mathrm{L}} = -\mathcal{A}^{-T}C^T v_{\mathrm{L}} \in \mathbb{R}_{++}^{n_{\widehat{x}}} \tag{6}$$

and $v_{\mathrm{L}} \in \mathbb{R}_{++}^N$ is a left-eigenvector of Ω with respect to the eigenvalue $1/\gamma$, i.e., v_{L} satisfies $v_{\mathrm{L}}^T\Omega = (1/\gamma)v_{\mathrm{L}}^T$. Namely, for any initial state $\widehat{x}(0) \in \mathbb{R}_+^{n_{\widehat{x}}} \setminus \{0\}$, we can achieve the convergence of output $\widehat{z}(t) = [\, z_1(t)\ \cdots\ z_N(t)\,]^T$ to $\gamma\alpha(\widehat{x}(0))v_{\mathrm{obj}} \in \mathbb{R}_{++}^N$.

This theorem implies that, for a given $v_{\mathrm{obj}} \in \mathbb{R}_{++}^N$ that represents the desired formation of N-agents, we can enforce their outputs (positions) to converge to (a positive scalar multiple of) v_{obj} by designing the interconnection matrix Ω so that the conditions (iii) and (iv) are satisfied. Even though we skip the technical details, this result can be seen as a generalization of a well-known consensus algorithm that has been basically applied to interconnected systems constructed from integrators [17]. See [20] for details.

3.2 Synthesis of Interconnected Matrices

It is meaningful to show a concrete way to design a desired $\Omega \in \mathbb{R}_+^{N\times N}$ satisfying $\Omega v_{\mathrm{obj}} = (1/\gamma)v_{\mathrm{obj}}$ and $\Gamma(\Omega) = \Gamma$ for a prescribed vector $v_{\mathrm{obj}} \in \mathbb{R}_{++}^N$ and a graph structure Γ. For illustration, we repeat the arguments in [15],[20] and consider the cases where Γ is schematically shown in Figs. 1 and 2 for $N = 3$.

For the graph structure Γ_{A}, any interconnection matrix $\Omega \in \mathbb{R}_+^{N\times N}$ satisfying $\Omega v_{\mathrm{obj}} = (1/\gamma)v_{\mathrm{obj}}$ and $\Gamma(\Omega) = \Gamma_{\mathrm{A}}$ can be parametrized by

$$\Omega = \frac{1}{\gamma}\Omega(v_{\mathrm{obj}}, p) \in \mathbb{R}_+^{N\times N} \tag{7}$$

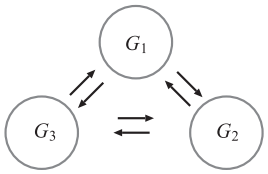

Fig. 1 Graph structure Γ_{A}.

Fig. 2 Graph structure Γ_{B}.

where

$$\Omega(v_{\mathrm{obj}},p)_{i,j}=\begin{cases}(1-p_1)\dfrac{v_{\mathrm{obj},1}}{v_{\mathrm{obj},N}} & (i,j)=(1,N),\\ p_i\dfrac{v_{\mathrm{obj},i}}{v_{\mathrm{obj},j}} & (1\le i\le N,\ j=i+1),\\ (1-p_i)\dfrac{v_{\mathrm{obj},i}}{v_{\mathrm{obj},j}} & (1\le i\le N,\ j=i-1),\\ p_N\dfrac{v_{\mathrm{obj},N}}{v_{\mathrm{obj},1}} & (i,j)=(N,1),\\ 0 & \text{otherwise.}\end{cases} \tag{8}$$

Here, the parameter vector $p\in\mathbb{R}^N_{++}$ can be chosen arbitrarily over $0<p<\mathbf{1}_N$ where $\mathbf{1}_N\in\mathbb{R}^N$ stands for the all-ones vector. On the other hand, for the graph structure Γ_B, any interconnection matrix $\Omega\in\mathbb{R}^{N\times N}_+$ satisfying $\Omega v_{\mathrm{obj}}=(1/\gamma)v_{\mathrm{obj}}$ and $\Gamma(\Omega)=\Gamma_{\mathrm{B}}$ can be parametrized again by (7) and (8) where $p\in\mathbb{R}^N_+$ can be chosen such that $p_1=1$, $p_N=0$, and $0<p_i<1$ ($i\in\mathbb{Z}_N\setminus\{1,N\}$). In both cases, we can confirm that the resulting interconnection matrix is irreducible (since Γ_{A} and Γ_{B} are both strongly connected). When $N=3$, matrices $\Omega(v_{\mathrm{obj}},p)$ for Γ_{A} and Γ_{B} can be given respectively as follows:

$\underline{\Gamma(\Omega)=\Gamma_{\mathrm{A}}}$

$$\Omega(v_{\mathrm{obj}},p)=\begin{bmatrix}0 & p_1\dfrac{v_{\mathrm{obj},1}}{v_{\mathrm{obj},2}} & (1-p_1)\dfrac{v_{\mathrm{obj},1}}{v_{\mathrm{obj},3}}\\ (1-p_2)\dfrac{v_{\mathrm{obj},2}}{v_{\mathrm{obj},1}} & 0 & p_2\dfrac{v_{\mathrm{obj},2}}{v_{\mathrm{obj},3}}\\ p_3\dfrac{v_{\mathrm{obj},3}}{v_{\mathrm{obj},1}} & (1-p_3)\dfrac{v_{\mathrm{obj},3}}{v_{\mathrm{obj},2}} & 0\end{bmatrix},$$

$\underline{\Gamma(\Omega)=\Gamma_{\mathrm{B}}}$

$$\Omega(v_{\mathrm{obj}},p)=\begin{bmatrix}0 & \dfrac{v_{\mathrm{obj},1}}{v_{\mathrm{obj},2}} & 0\\ (1-p_2)\dfrac{v_{\mathrm{obj},2}}{v_{\mathrm{obj},1}} & 0 & p_2\dfrac{v_{\mathrm{obj},2}}{v_{\mathrm{obj},3}}\\ 0 & \dfrac{v_{\mathrm{obj},3}}{v_{\mathrm{obj},2}} & 0\end{bmatrix}.$$

We finally note that the eigenvalues of $\Omega(v_{\mathrm{obj}},p)\in\mathbb{R}^{N\times N}_+$ depend solely on $p\in\mathbb{R}^N_+$ and do not depend on $v_{\mathrm{obj}}\in\mathbb{R}^N_{++}$. This can be easily confirmed if we note

$$\begin{aligned}\Omega(v_{\mathrm{obj}},p) &= \mathrm{diag}(v_{\mathrm{obj},1},\cdots,v_{\mathrm{obj},N})\Omega(\mathbf{1}_N,p)\\ &\quad\times\mathrm{diag}(v_{\mathrm{obj},1},\cdots,v_{\mathrm{obj},N})^{-1}.\end{aligned}$$

3.3 Concrete Examples of Formation Control

In this section, we show that a practical formation control problem can be cast as a formation control problem of multi-agent positive systems as discussed in the preceding subsections. Consider the formation control problem of N agents that move over the (x,y)-plane. We denote by $(z_{i,x}(t),z_{i,y}(t))$ the position of agent i. Furthermore, we define $\widehat{z}_j:=[z_{1,j}\ \cdots\ z_{N,j}]^T$ $(j=x,y)$ by stacking the coordinates of all agents.

We assume that agent i has independent dynamics along the x- and y-axes, denoted by $P_{i,x}(s)$ and $P_{i,y}(s)$, respectively, and independent control inputs $u_{i,x}(t)$ and $u_{i,y}(t)$. Suppose $P_{i,x}(s)$ and $P_{i,y}(s)$ are typical dynamics of moving agents given by

$$\begin{aligned}&Z_{i,j}(s)=P_{i,j}(s)U_{i,j}(s),\\ &P_{i,j}(s)=\frac{k_{i,j}}{s(s+a_{i,j})}\ (i\in\mathbb{Z}_N,\ j=x,y)\end{aligned}$$

where $k_{i,j},a_{i,j}>0$. Roughly speaking, our goal here is to design communication schemes (interconnection matrices) over N-agents along x- and y-axes independently so that prescribed formation can be achieved asymptotically.

Before designing interconnection matrices over the agents, we apply the local feedback

$$u_{i,j}(t)=-f_{i,j}(z_{i,j}(t)-w_{i,j}(t))\ (i\in\mathbb{Z}_N,\ j=x,y)$$

with $0<f_{i,j}\le a_{i,j}^2/4k_{i,j}$, where $w_{i,j}$ $(i\in\mathbb{Z}_N,\ j=x,y)$ is the exogenous input kept for the interconnection. Then we have

$$\begin{aligned}&Z_{i,j}(s)=G_{i,j}(s)W_{i,j}(s),\\ &G_{i,j}(s)=\left[\begin{array}{cc|c}-b_{i,j} & 1 & 0\\ 0 & -c_{i,j} & b_{i,j}c_{i,j}\\ \hline 1 & 0 & 0\end{array}\right],\\ &b_{i,j}+c_{i,j}=a_{i,j},\ b_{i,j}c_{i,j}=f_{i,j}k_{i,j}.\end{aligned} \tag{9}$$

It follows that $G_{i,j}$ $(i\in\mathbb{Z}_N,\ j=x,y)$ are stable positive systems (in the realization (9)) with $G_{i,j}(0)=1$ $(i\in\mathbb{Z}_N,\ j=x,y)$. The latter property is a natural consequence from the fact that each open-loop transfer function $P_{i,j}(s)$ $(i\in\mathbb{Z}_N,\ j=x,y)$ includes an integrator. For description simplicity, we define $\widehat{w}_j:=[w_{1,j}\ \cdots\ w_{N,j}]^T$ $(j=x,y)$.

Suppose that N-agents independently communicate their x and y positions. Then, we can restate our goal as in designing Ω_x and Ω_y such that, under the interconnection with Ω_x and Ω_y for $(\widehat{z}_x,\widehat{w}_x)$ and $(\widehat{z}_y,\widehat{w}_y)$, respectively, the following formation can be achieved:

$$\lim_{t\to\infty}[\,\widehat{z}_x(t)\,\widehat{z}_y(t)\,]=[\,\alpha_x(\widehat{x}_x(0))v_{\mathrm{obj},x}\ \alpha_y(\widehat{x}_y(0))v_{\mathrm{obj},y}\,]. \tag{10}$$

Here, $(v_{\mathrm{obj},x},v_{\mathrm{obj},y})$ are given vectors that specify the desired formation. On the other hand, $\widehat{x}_x(0)$ and $\widehat{x}_y(0)$ stand for the initial states of the corresponding interconnected systems, and α_x and α_y are linear functions. It is obvious that we can readily solve this problem by following Theorem 1.

For a concrete and concise illustration, consider the case where the dynamics are homogeneous over the agents and (x,y)-coordinates as well by letting $a_{i,j}=a=50$, $k_{i,j}=k=1$ and $f_{i,j}=0.8\times a^2/4k$ $(i\in\mathbb{Z}_N,\ j=x,y)$. We let $N=20$ and

$$\left[v_{\mathrm{obj},x}\ v_{\mathrm{obj},y}\right]_i=[2+\cos(2\pi i/N)\quad 2+\sin(2\pi i/N)]\,.$$

Namely, the vectors $(v_{\mathrm{obj},x},v_{\mathrm{obj},y})$ are chosen to form a circle. Under this setting, we designed two pairs of $(\Omega_{\mathrm{A},x},\Omega_{\mathrm{A},y})$ and $(\Omega_{\mathrm{B},x},\Omega_{\mathrm{B},y})$ detailed below:

(A) $\Gamma(\Omega_{\mathrm{A},x})=\Gamma(\Omega_{\mathrm{A},y})=\Gamma_{\mathrm{A}}$,
$\Omega_{\mathrm{A},x}=\Omega(v_{\mathrm{obj},x},p_{\mathrm{A},x})$, $\Omega_{\mathrm{A},y}=\Omega(v_{\mathrm{obj},y},p_{\mathrm{A},y})$.

(B) $\Gamma(\Omega_{\mathrm{B},x}) = \Gamma(\Omega_{\mathrm{B},y}) = \Gamma_{\mathrm{B}}$,
$\Omega_{\mathrm{B},x} = \Omega(v_{\mathrm{obj},x}, p_{\mathrm{B},x})$, $\Omega_{\mathrm{B},y} = \Omega(v_{\mathrm{obj},y}, p_{\mathrm{B},y})$.

Here we choose parameters $p_{\mathrm{A},x} \in \mathbb{R}^N_{++}$ and $p_{\mathrm{B},x} \in \mathbb{R}^N_{+}$ so that there exists $v_{\mathrm{L},x} \in \mathbb{R}^N_{++}$ satisfying

$$v^T_{\mathrm{L},x}\Omega(v_{\mathrm{obj},x}, p_{\mathrm{A},x}) = v^T_{\mathrm{L},x}\Omega(v_{\mathrm{obj},x}, p_{\mathrm{B},x}) = v^T_{\mathrm{L},x}.$$

Similarly, we choose parameters $p_{\mathrm{A},y} \in \mathbb{R}^N_{++}$ and $p_{\mathrm{B},y} \in \mathbb{R}^N_{+}$ so that there exists $v_{\mathrm{L},y} \in \mathbb{R}^N_{++}$ satisfying

$$v^T_{\mathrm{L},y}\Omega(v_{\mathrm{obj},y}, p_{\mathrm{A},y}) = v^T_{\mathrm{L},y}\Omega(v_{\mathrm{obj},y}, p_{\mathrm{B},y}) = v^T_{\mathrm{L},y}.$$

Such parameters can be computed by solving linear equations along the line in [15]. From (6), we can confirm that the output $[\widehat{z}_x(t)\ \widehat{z}_y(t)]$ converges to the same value under the interconnections $(\Omega_{\mathrm{A},x}, \Omega_{\mathrm{A},y})$ and $(\Omega_{\mathrm{B},x}, \Omega_{\mathrm{B},y})$.

In Figs. 3–10, we show the plots of $[\widehat{z}_x(t)\ \widehat{z}_y(t)]$ for the cases (A) and (B). In both cases, we took exactly the same initial states as implied by Figs. 3 and 7. In both cases, we successfully achieved exactly the same circular formation (scaled along x- and y-axes independently) as expected. However, the convergence performance is quite different between (A) and (B): it is clear from Figs. 4 and 8 that the convergence of case (A) is much faster than case (B).

Note that the dynamics of $\mathcal{G} \star \Omega$ can be represented by $\dot{\widehat{x}} = (\mathcal{A} + \mathcal{B}\Omega\mathcal{C})\widehat{x}$. Then, if the system $\mathcal{G} \star \Omega$ is under formation control, i.e., if the conditions (i)–(iv) in Theorem 1 are satisfied, we know from [15],[20] that the matrix $\mathcal{A} + \mathcal{B}\Omega\mathcal{C}$ has eigenvalue 0 that is algebraically simple, and the real parts of the other eigenvalues are strictly negative. Therefore, the real part of the dominant pole of $\mathcal{G} \star \Omega$, i.e., the second largest real part of the eigenvalues of $\mathcal{A} + \mathcal{B}\Omega\mathcal{C}$ denoted by $\kappa_2(\mathcal{A} + \mathcal{B}\Omega\mathcal{C})$, is a reasonable measure for the convergence rate performance. Of course the computation of the dominant pole can be done by simply computing all the eigenvalues of $\mathcal{A} + \mathcal{B}\Omega\mathcal{C}$ and comparing their real parts. By this simple procedure, we know in the above examples that

$$\begin{aligned}&(\kappa_2(\mathcal{A} + \mathcal{B}\Omega_{\mathrm{A},x}\mathcal{C}), \kappa_2(\mathcal{A} + \mathcal{B}\Omega_{\mathrm{A},y}\mathcal{C}))\\ &= (-0.3719, -0.4890)\\ &(\kappa_2(\mathcal{A} + \mathcal{B}\Omega_{\mathrm{B},x}\mathcal{C}), \kappa_2(\mathcal{A} + \mathcal{B}\Omega_{\mathrm{B},y}\mathcal{C}))\\ &= (-0.0951, -0.1501).\end{aligned} \tag{11}$$

These results surely validates the fact that the convergence of case (A) is much faster than case (B).

Even though we obtained (11) by directly computing all the eigenvalues of $\mathcal{A} + \mathcal{B}\Omega\mathcal{C}$, such a straightforward method is computationally demanding especially when the total number of agents becomes larger. Moreover, such a method does not give any insights on how we can accelerate the convergence by appropriately designing Ω. Motivated by these facts, in the next section, we propose an efficient algorithm for the computation of $\kappa_2(\mathcal{A}+\mathcal{B}\Omega\mathcal{C})$ by decomposing the original large size problem into small size problems and exploiting the positive property of each agent. Note that the real part of the dominant pole is often called algebraic connectivity in the study area of multi-agent systems [17]–[19],[22],[23]. In the case where the dynamics of agents are simple as in the case of integrators, the algebraic connectivity can be determined solely by the interconnection matrix but this is not the case in general. Our objective is to establish an efficient algorithm by exploiting the positive property of each agent.

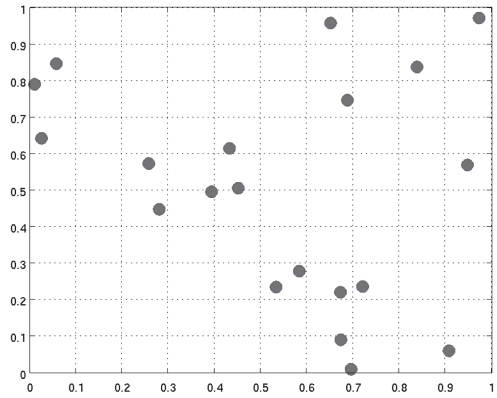

Fig. 3 $[\widehat{z}_x(t)\ \widehat{z}_y(t)]$ for $t = 0$ s under $(\Omega_{\mathrm{A},x}, \Omega_{\mathrm{A},y})$.

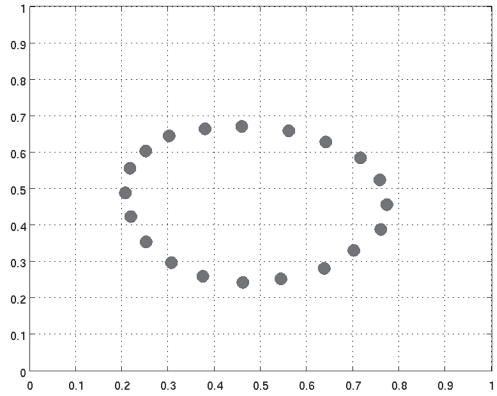

Fig. 4 $[\widehat{z}_x(t)\ \widehat{z}_y(t)]$ for $t = 10$ s under $(\Omega_{\mathrm{A},x}, \Omega_{\mathrm{A},y})$.

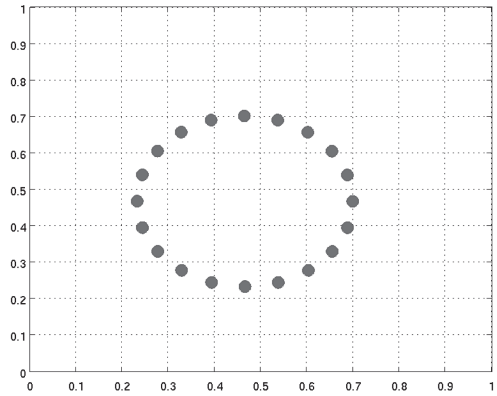

Fig. 5 $[\widehat{z}_x(t)\ \widehat{z}_y(t)]$ for $t = 20$ s under $(\Omega_{\mathrm{A},x}, \Omega_{\mathrm{A},y})$.

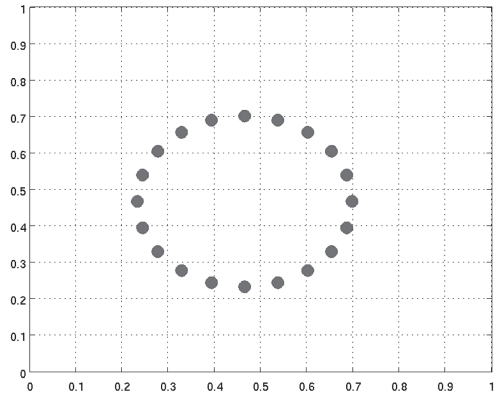

Fig. 6 $[\widehat{z}_x(t)\ \widehat{z}_y(t)]$ for $t = 30$ s under $(\Omega_{\mathrm{A},x}, \Omega_{\mathrm{A},y})$.

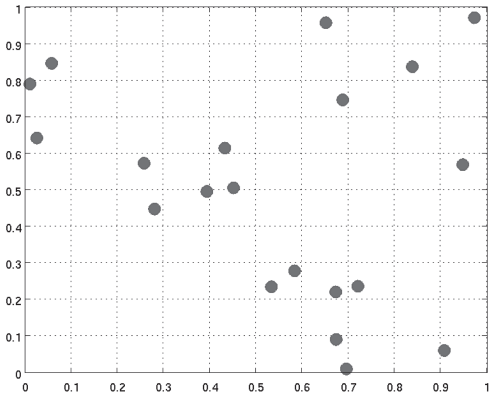

Fig. 7 $[\widehat{z}_x(t)\,\widehat{z}_y(t)]$ for $t = 0$ s under $(\Omega_{\mathrm{B},x}, \Omega_{\mathrm{B},y})$.

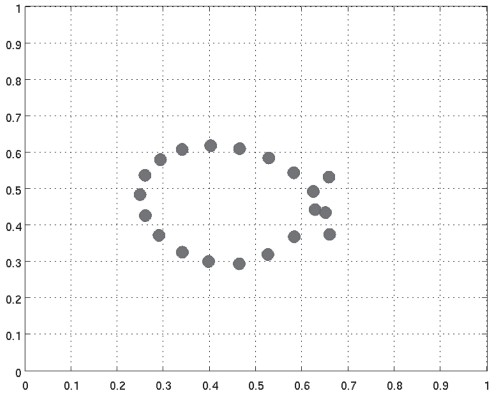

Fig. 8 $[\widehat{z}_x(t)\,\widehat{z}_y(t)]$ for $t = 10$ s under $(\Omega_{\mathrm{B},x}, \Omega_{\mathrm{B},y})$.

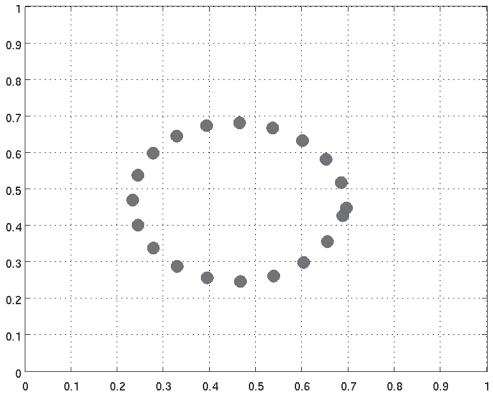

Fig. 9 $[\widehat{z}_x(t)\,\widehat{z}_y(t)]$ for $t = 20$ s under $(\Omega_{\mathrm{B},x}, \Omega_{\mathrm{B},y})$.

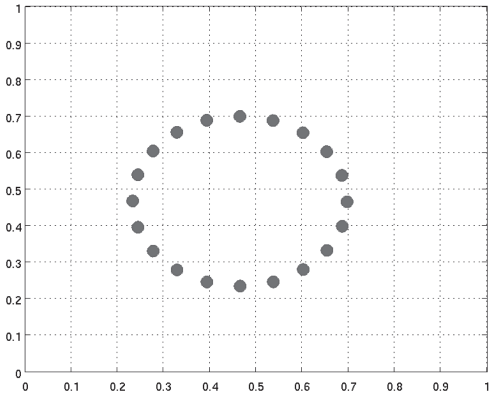

Fig. 10 $[\widehat{z}_x(t)\,\widehat{z}_y(t)]$ for $t = 30$ s under $(\Omega_{\mathrm{B},x}, \Omega_{\mathrm{B},y})$.

From now on we assume that the dynamics of all agents are homogeneous. This assumption is indispensable in constructing the efficient algorithm.

Remark 1 Before getting into the details of the efficient algorithm, we give some remarks on the simulation results shown in Figs. 3–10. In these examples, since the interconnected systems along x- and y-axes are both positive, and since we chose the initial states $\widehat{x}_x(0)$ and $\widehat{x}_y(0)$ to be both positive, the moving region of agents is limited to the first quadrant. If we do not restrict $\widehat{x}_x(0)$ and/or $\widehat{x}_y(0)$ to be positive, however, it is of course true that the agents can go outside the first quadrant and satisfy (10). These are obvious from the linearity of the dynamics along x- and y-axes. The positivity of agents under formation control would be useful for those cases where the allowable moving region of agents is physically restricted to be the first quadrant (possibly with appropriate coordinate changes).

4. Efficient Algorithms for the Computation of $\kappa_2(\mathcal{A}+\mathcal{B}\Omega\mathcal{C})$

In this section, we propose an efficient algorithm for the computation of (the real part of) the dominant pole of multi-agent positive systems under formation control. As noted previously, we assume that the dynamics of all agents are homogeneous and thus

$$\begin{aligned} &A_i = A \in \mathbb{M}^n \cap \mathbb{H}^n,\ B_i = B \in \mathbb{R}_+^{n\times 1},\\ &C_i = C \in \mathbb{R}_+^{1\times n}\ (i \in \mathbb{Z}_N) \end{aligned} \tag{12}$$

holds in (2). In the following we further assume that $G_i = G$ $(i \in \mathbb{Z}_N)$ and $\Omega \in \mathbb{R}_+^{N\times N}$ satisfy the conditions (i)–(iv) in Theorem 1 with $\gamma = 1$ (as in Subsection 3.3).

4.1 Basic Algorithm by Problem Decomposition

The next lemma is instrumental for the decomposition of the computation of $\kappa_2(\mathcal{A} + \mathcal{B}\Omega\mathcal{C})$ into smaller size computation problems. We do not claim that this lemma is new, and similar results can be found, for instance, in [24]. Still, we give the proof for the completeness of the discussion.

Lemma 1 For given $\Omega \in \mathbb{R}^{N\times N}$ and $\mathcal{P}, \mathcal{Q} \in \mathbb{R}^{m\times m}$, we have

$$\sigma\left(I_N \otimes \mathcal{P} + \Omega \otimes \mathcal{Q}\right) = \left\{\lambda \in \sigma(\mathcal{P} + \nu\mathcal{Q}) : \nu \in \sigma(\Omega)\right\}. \tag{13}$$

Proof of Lemma 1: The Schur's unitary triangularization theorem [Theorem 2.3.1 of [4]] ensures that there exists a unitary matrix $U \in \mathbb{C}^{n\times n}$ such that $U^*\Omega U (=: \Delta_\Omega)$ is upper triangular. By applying a similarity transformation with this U, we have

$$\begin{aligned} &(U \otimes I_m)^* (I_n \otimes \mathcal{P} + \Omega \otimes \mathcal{Q})(U \otimes I_m)\\ &= (I_n \otimes \mathcal{P} + \Delta_\Omega \otimes \mathcal{Q})\\ &= \begin{bmatrix} \mathcal{P}+\nu_1\mathcal{Q} & * & \cdots & \cdots & * \\ 0 & \mathcal{P}+\nu_2\mathcal{Q} & \ddots & & \vdots \\ \vdots & \ddots & \ddots & \ddots & \vdots \\ \vdots & & \ddots & \ddots & * \\ 0 & \cdots & \cdots & 0 & \mathcal{P}+\nu_n\mathcal{Q} \end{bmatrix} \end{aligned}$$

where $\sigma(\Omega) = \{\nu_1, \cdots, \nu_n\}$ including algebraic multiplicities. The above equality clearly shows that (13) holds. ■

The next result readily follows from Lemma 1.

Proposition 2 For given $\Omega \in \mathbb{R}^{N\times N}$ and $\mathcal{A} \in \mathbb{M}^{Nn}$, $\mathcal{B} \in \mathbb{R}_+^{Nn\times N}$, $\mathcal{C} \in \mathbb{R}_+^{N\times Nn}$ given by (2), (4) and (12), we have

$$\sigma(\mathcal{A} + \mathcal{B}\Omega\mathcal{C}) = \{\lambda \in \sigma(A + \nu BC) : \nu \in \sigma(\Omega)\}. \quad (14)$$

Proof of Proposition 2: Note that

$$\begin{aligned}\mathcal{A} + \mathcal{B}\Omega\mathcal{C} &= I_N \otimes A + (I_N \otimes B)\Omega(I_N \otimes C)\\ &= I_N \otimes A + (I_N \otimes B)(\Omega \otimes C)\\ &= I_N \otimes A + \Omega \otimes BC.\end{aligned}$$

Therefore (14) holds from Lemma 1. ■

Note that Proposition 2 holds only if G is SISO. This proposition implies that we can compute the eigenvalues of $\mathcal{A}+\mathcal{B}\Omega\mathcal{C} \in \mathbb{R}^{Nn\times Nn}$ by computing the eigenvalues of $A + \nu_i BC \in \mathbb{R}^{n\times n}$ repeatedly over $\nu_i \in \sigma(\Omega)$. Based on this fact, we can conceive the following algorithm that is expected to be efficient if N is large.

Algorithm I (Basic Algorithm)

Step 0: Sort the distinct eigenvalues of Ω with nonnegative imaginary part in descending order with respect to their absolute values and denote them by $\lambda_1, \cdots, \lambda_M$ ($M \le N$). From the underlying assumption on Ω we have $\lambda_1 = 1$.

Step 1: Let $\kappa^\star = \kappa_2(A + \lambda_1 BC) = \kappa_2(A + BC)$ and $i = 2$.

Step 2: Compute $\kappa(\lambda_i) := \kappa(A + \lambda_i BC)$ and let $\kappa^\star := \max(\kappa(\lambda_i), \kappa^\star)$.

Step 3: If $i = M$, exit. Else, let $i := i + 1$ and go to Step 2.

The efficiency of this algorithm can be validated by the computational complexity analysis results in matrix eigenvalue computation. When we deal with the eigenvalue computation of a matrix of size n, the computational complexity is $O(n^3)$ for the reduction to Hessenberg form, and $O(n^2)$ for a single step in QR iteration [25]. Therefore, Algorithm I is expected to be very efficient since it reduces the size of the matrix to be examined from Nn to n.

Still, in Algorithm I, we need to compute the eigenvalues of $A + \lambda_i BC$ repeatedly over $i \in \mathbb{Z}_M$ and thus this algorithm leaves room for improvement. In fact, if we focus on the positivity of G, i.e., if we exploit the fact that $A \in \mathbb{M}^n$, $B \in \mathbb{R}_+^n$ and $C \in \mathbb{R}_+^{1\times n}$, we can drastically reduce the number of eigenvalues $\lambda_i \in \sigma(\Omega)$ to be examined. This is the key idea for conceiving a much more efficient algorithm as detailed in the next subsection.

4.2 Efficient Algorithm by Exploiting Positivity

The next theorem is very important for enhancing the efficiency of Algorithm I.

Theorem 2 For given $A, B \in \mathbb{R}_+^{n\times n}$, we have

$$\rho(A + \nu B) \le \rho(A + B) \quad \forall \nu \in \mathbb{D}. \quad (15)$$

The proof of this theorem is given in the appendix. As noted in Section 1, the proof relies on strong results on stability and H_∞ norm of (discrete-time) positive systems and clearly illustrate how positivity of subsystems can be exploited to conceive the efficient algorithm.

Next corollary follows directly from this theorem.

Corollary 1 For given $A \in \mathbb{M}^n$ and $B \in \mathbb{R}_+^{n\times n}$, we have

$$\kappa(A + \nu B) \le \kappa(A + B) \quad \forall \nu \in \mathbb{D}. \quad (16)$$

Proof of Corollary 1: Since $A \in \mathbb{M}^n$, there exists $\alpha \in \mathbb{R}$ such that $A + \alpha I \in \mathbb{R}_+^{n\times n}$. Then, from Theorem 2 and the facts that $\kappa(M) \le \rho(M)$ for $M \in \mathbb{C}^{n\times n}$ and $\rho(M) = \kappa(M)$ for $M \in \mathbb{R}_+^{n\times n}$ [4], we have for any $\nu \in \mathbb{D}$ that

$$\begin{aligned}\kappa(A + \alpha I + \nu B) &\le \rho(A + \alpha I + \nu B)\\ &\le \rho(A + \alpha I + B)\\ &= \kappa(A + \alpha I + B)\end{aligned}$$

where we used (15) to prove the second inequality. This clearly shows that (16) holds. ■

In relation to the computation of $\kappa_2(\mathcal{A} + \mathcal{B}\Omega\mathcal{C})$ along the line of Algorithm I, Corollary 1 shows that we can reduce the number of eigenvalues $\lambda_i \in \sigma(\Omega)$ to be examined. Indeed, by paying attention to the fact that $\lambda_1, \ldots, \lambda_M$ ($M \le N$) are sorted in descending order with respect to their absolute values, we can include the following stopping condition to Algorithm I:

(i) If $\overline{\kappa}(\lambda_i) := \kappa(A + |\lambda_i|BC)$ is not larger than the tentative value $\kappa^\star$, we can let $\kappa_2(\mathcal{A} + \mathcal{B}\Omega\mathcal{C}) = \kappa^\star$ and exit the algorithm.

(ii) If $\lambda_i \in \mathbb{R}_{++}$, we can let $\kappa_2(\mathcal{A} + \mathcal{B}\Omega\mathcal{C}) = \max(\kappa^\star, \kappa(A + \lambda_i BC))$ and exit the algorithm.

We are now ready to give the efficient algorithm for the computation of $\kappa_2(\mathcal{A} + \mathcal{B}\Omega\mathcal{C})$.

Algorithm II (Efficient Algorithm)

Steps 0 and 1: The same as Algorithm I.

Step 2: Compute $\overline{\kappa}(\lambda_i) := \kappa(A + |\lambda_i|BC)$. If $\overline{\kappa}(\lambda_i) \le \kappa^\star$, exit. If $\lambda_i \in \mathbb{R}_{++}$, let $\kappa^\star := \max(\overline{\kappa}(\lambda_i), \kappa^\star)$ and exit. Else, go to Step 3.

Step 3: Compute $\kappa(\lambda_i) := \kappa(A + \lambda_i BC)$ and let $\kappa^\star := \max(\kappa(\lambda_i), \kappa^\star)$.

Step 4: If $i = M$, exit. Else, let $i := i + 1$ and go to Step 2.

Algorithm II is efficient particularly when $\Omega \in \mathbb{R}_+^{N\times N}$ has only real eigenvalues (e.g., this happens when Ω is symmetric). In such a case, if Ω has a positive eigenvalue λ, then we do not need to test the eigenvalues whose absolute values are less than or equal to λ. By following this line, we can analytically write down $\kappa_2(\mathcal{A} + \mathcal{B}\Omega\mathcal{C})$ for some specific interconnection matrices.

For example, consider the interconnection matrix $\Omega_{A,0} := \Omega(\mathbf{1}_N, p_{A,0})$ where $p_{A,0} := \frac{1}{2}\mathbf{1}_N$. In this case, $\Gamma(\Omega_{A,0}) = \Gamma_A$ holds and

$$\sigma(\Omega_{A,0}) = \left\{\cos\left(\frac{2\pi(i-1)}{N}\right) : i \in \mathbb{Z}_N\right\}. \quad (17)$$

It follows that

$$\kappa_2(\mathcal{A} + \mathcal{B}\Omega_{A,0}C) = \begin{cases}\max\left(\kappa_2(A + BC), \kappa(A + \lambda_2 BC), \kappa(A + \lambda_{K+1}BC)\right)\\ \quad N = 2K + 1\\ \max\left(\kappa_2(A + BC), \kappa(A + \lambda_2 BC), \kappa(A - BC)\right)\\ \quad N = 2K\end{cases} \quad (18)$$

where $K \in \mathbb{Z}_+$ and

$$\lambda_2 := \cos\left(\frac{2\pi}{N}\right),\ \lambda_{K+1} := \cos\left(\frac{2K\pi}{2K+1}\right).$$

On the other hand, we see that $\Omega_{B,0} := \Omega(\mathbf{1}_N, p_{B,0})$ with $p_{B,0} := [\ 1\ \frac{1}{2}\mathbf{1}_{N-2}^T\ 0\ ]^T$ satisfies $\gamma(\Omega_{B,0}) = \Gamma_B$ and

Table 1 Average CPU time ($n = 2$).

N	Algorithm 0	Algorithm I	Algorithm II
10	0.3907×10^{-3}	0.2983×10^{-3}	0.2541×10^{-3}
100	0.0319	0.0074	0.0065
1000	8.4881	1.2354	1.2269

Table 2 Average CPU time ($n = 3$).

N	Algorithm 0	Algorithm I	Algorithm II
10	0.5488×10^{-3}	0.3709×10^{-3}	0.2798×10^{-3}
100	0.0756	0.0076	0.0067
1000	27.9230	1.2339	1.2230

Table 3 Average CPU time of Algorithms I and II ($n = 2$).

N	Steps 0,1	Algorithm I Steps 2, 3	Algorithm II Steps 2, 3, 4
10	0.1647×10^{-3}	0.1336×10^{-3}	0.0894×10^{-3}
100	0.0064	0.9208×10^{-3}	0.1205×10^{-3}
1000	1.2266	0.0088	0.0003

Table 4 Average CPU time of Algorithms I and II ($n = 3$).

N	Steps 0, 1	Algorithm I Steps 2, 3	Algorithm II Steps 2, 3, 4
10	0.1786×10^{-3}	0.1923×10^{-3}	0.1012×10^{-3}
100	0.0067	0.0012	0.0002
1000	1.2225	0.0114	0.0004

$$\sigma(\Omega_{\mathrm{B},0}) = \left\{ \cos\left(\frac{\pi(i-1)}{N-1}\right) : i \in \mathbb{Z}_N \right\} \tag{19}$$

for $N \geq 3$. Therefore we have

$$\begin{aligned} &\kappa_2(\mathcal{A} + \mathcal{B}\Omega_{\mathrm{B},0}\mathcal{C}) \\ &= \max\left(\kappa_2(A+BC), \kappa(A-BC), \kappa\left(A + \cos\left(\tfrac{\pi}{N-1}\right)BC\right)\right). \end{aligned} \tag{20}$$

It follows that in the cases $\Omega = \Omega_{\mathrm{A},0}$ and $\Omega = \Omega_{\mathrm{B},0}$ we can compute $\kappa_2(\mathcal{A} + \mathcal{B}\Omega\mathcal{C})$ very efficiently irrespective of N.

5. Numerical Examples

In this section, we demonstrate the efficiency of Algorithms I and II by numerical examples. For given n and N, we randomly generated $A \in \mathbb{M}^n \cap \mathbb{H}^n$, $B \in \mathbb{R}_+^{n\times 1}$ and $C \in \mathbb{R}_+^{1\times n}$ ($i \in \mathbb{Z}_N$) satisfying $G(0) = -CA^{-1}B = 1$ and irreducible $\Omega \in \mathbb{R}_+^{N\times N}$ satisfying $\lambda_{\mathrm{F}}(\Omega) = 1$. Then, we computed $\kappa_2(\mathcal{A} + \mathcal{B}\Omega\mathcal{C})$ by direct computation of $\sigma(\mathcal{A} + \mathcal{B}\Omega\mathcal{C})$ (this method is denoted by Algorithm 0 for simplicity) and Algorithms I and II. The average computation time over 10 tested cases for each setting $N = 10, 100, 1000$ with $n = 2$ and 3 are shown in Tables 1 and 2, respectively (in Tables 1–4, the unit for CPU time is second). These tables show that Algorithms I and II are much more efficient than Algorithm 0. This is due to the fact that in Algorithms I and II we can avoid the eigenvalue computation of matrices of large size Nn.

On the other hand, from these tables we cannot see clearly the efficiency of Algorithm II over Algorithm I. This is due to the fact that in both algorithms most of computation time is consumed by the common steps, Steps 0 and 1, i.e., the computation of the eigenvalues of Ω. To compare the efficiency of Algorithms I and II in more detail, we show in Tables 3 and 4 the computation times of Algorithm I needed for Steps 0 and 1, and for the remaining steps, Steps 2 and 3. Similarly, we show in these tables the computation times of Algorithm II needed for Steps 0 and 1, and for the remaining steps, Steps 2, 3, and 4. From these tables, it is clear that Algorithm II consumes very little time for the Steps 2, 3, and 4, i.e., the computation of the eigenvalues $A + \lambda_i BC$ over $\lambda_i \in \sigma(\Omega)$ that have to be examined. To highlight this point, we show in Tables 5 and 6 the average number of the eigenvalues of Ω examined in Algorithms I and II. It is clear that Algorithm II successfully reduce the number of eigenvalues to be examined by including stopping conditions (i) and (ii) stated in Subsection 4.2. To summarize, even though computation time reduction of Algorithm II over Algorithm I is not significant, Algorithm II is efficient and reasonable in avoiding unnecessary computations.

Table 5 Average number of examined eigenvalues of Ω ($n = 2$).

N	Algorithm I	Algorithm II
10	7.4	3.2
100	54.6	7.9
1000	514.2	13.3

Table 6 Average number of examined eigenvalues of Ω ($n = 3$).

N	Algorithm I	Algorithm II
10	7.0	3.4
100	54.8	7.3
1000	512.6	12.2

6. Conclusion

In this paper, we proposed an efficient algorithm for the convergence rate analysis of multi-agent positive systems under formation control. Assuming that the dynamics of all agents are positive and homogeneous, we first showed that the dominant pole of the overall interconnected positive system can be computed by evaluating eigenvalues of matrices whose sizes are equal to the dimension of each subsystem. Then, by actively using positive property of each subsystem, we showed that we can drastically decrease the number of matrices to be examined. We illustrated by numerical examples that the proposed algorithm is definitely efficient.

References

[1] L. Farina and S. Rinaldi: *Positive Linear Systems: Theory and Applications*, John Wiley and Sons, 2000.

[2] T. Kaczorek: *Positive 1D and 2D Systems*, Springer, London, 2001.

[3] A. Berman and R.J. Plemmons: *Nonnegative Matrices in the Mathematical Sciences*, Academic Press, New York, 1979.

[4] R.A. Horn and C.A. Johnson: *Matrix Analysis*, Cambridge University Press, New York, 1985.

[5] R.A. Horn and C.A. Johnson: *Topics in Matrix Analysis*, Cambridge University Press, New York, 1991.

[6] O. Mason and R. Shorten: On linear copositive Lyapunov function and the stability of switched positive linear systems, *IEEE Transactions on Automatic Control*, Vol. 52, No. 7, pp. 1346–1349, 2007.

[7] A. Rantzer: Distributed control of positive systems, *Proc. Conference on Decision and Control*, pp. 6608–6611, 2011.

[8] A. Rantzer: On the Kalman-Yakubovich-Popov lemma for positive systems, *Proc. Conference on Decision and Control*, pp. 7482–7484, 2012.

[9] T. Tanaka and C. Langbort: The bounded real lemma for internally positive systems and H_∞ structured static state feedback, *IEEE Transactions on Automatic Control*, Vol. 56, No. 9, pp. 2218–2223, 2011.

[10] F. Blanchini, P. Colaneri, and M.E. Valcher: Co-positive

Lyapunov functions for the stabilization of positive switched systems, *IEEE Transactions on Automatic Control*, Vol. 57, No. 12, pp. 3038–3050, 2012.
[11] Y. Ebihara, D. Peaucelle, and D. Arzelier: LMI approach to linear positive system analysis and synthesis, *Systems and Control Letters*, Vol. 63, No. 1, pp. 50–56, 2014.
[12] M.E. Valcher and P. Misra: On the stabilizability and consensus of positive homogeneous multi-agent dynamical systems, *IEEE Transactions on Automatic Control*, Vol. 59, No. 7, pp. 1936–1941, 2014.
[13] Y. Ebihara, D. Peaucelle, and D. Arzelier: L_1 gain analysis of linear positive systems and its application, *Proc. Conference on Decision and Control*, pp. 4029–4034, 2011.
[14] Y. Ebihara, D. Peaucelle, and D. Arzelier: Decentralized control of interconnected positive systems using L_1-induced norm characterization, *Proc. Conference on Decision and Control*, pp. 6653–6658, 2012.
[15] Y. Ebihara, D. Peaucelle, and D. Arzelier: Stability and persistence analysis of large scale interconnected positive systems, *Proc. European Control Conference*, pp. 3366–3371, 2013.
[16] Y. Ebihara, D. Peaucelle, and D. Arzelier: Analysis and synthesis of interconnected SISO positive systems with switching, *Proc. Conference on Decision and Control*, pp. 6372–6378, 2013.
[17] R. Olfati-Saber, J.A. Fax, and R.M. Murray: Consensus and cooperation in networked multi-agent systems, *Proc. IEEE*, Vol. 95, No. 1, pp. 215–233, 2007.
[18] H.G. Tanner, A. Jadbabaie, and G.J. Pappas: Stable flocking of mobile agents, part I: Fixed topology, *Proc. Conference on Decision and Control*, pp. 2010–2015, 2003.
[19] H.G. Tanner, A. Jadbabaie, and G.J. Pappas: Stable flocking of mobile agents, part II: Dynamic topology, *Proc. Conference on Decision and Control*, pp. 2016–2021, 2003.
[20] Y. Ebihara, D. Peaucelle, and D. Arzelier: Analysis and synthesis of interconnected positive systems, *IEEE Transactions on Automatic Control*, to appear, 2017.
[21] Y. Ebihara, D. Peaucelle, and D. Arzelier: Efficient convergence rate analysis of multi-agent positive systems under formation control, *Proc. 19th IFAC World Congress*, pp. 3790–3796, 2014.
[22] M. Fujita and T. Hatanaka: Cooperative control: Basic results on consensus and coverage control problems, *Proc. 52nd Annual Conference of the ISCIE*, pp. 1–6, 2008 (in Japanese).
[23] R. Olfati-Saber and R.M. Murray: Consensus problems in networks of agents with switching topology and time-delays, *IEEE Transactions on Automatic Control*, Vol. 49, No. 9, pp. 1520–1533, 2004.
[24] P.A. Fuhrmann and U. Helmke: *The Mathematics of Networks of Linear Systems*, Springer, Switzerland, 2015.
[25] G.H. Golub and C.F.V. Loan: *Matrix Computations*, The Johns Hopkins University Press, Baltimore, 1996.
[26] F. Najson: On the Kalman-Yakubovich-Popov lemma for discrete-time positive linear systems: A novel simple proof and some related results, *International Journal of Control*, Vol. 86, No. 10, pp. 1813–1823, 2013.
[27] A. Rantzer: On the Kalman-Yakubovich-Popov lemma, *Systems and Control Letters*, Vol. 28, No. 1, pp. 7–10, 1996.

Appendix A Proof of Theorem 2

Proof of Theorem 2: It suffices to prove that

$$\rho(A+B)<\gamma \;\Rightarrow\; \rho(A+\nu B)<\gamma \quad \forall \nu\in\mathbb{D}. \tag{A.1}$$

This can be rewritten equivalently as

$$\rho(A_\gamma+B_\gamma)<1 \;\Rightarrow\; \rho(A_\gamma+\nu B_\gamma)<1 \quad \forall \nu\in\mathbb{D}$$

where $A_\gamma := A/\gamma$ and $B_\gamma := B/\gamma$. Therefore, for the proof of Theorem 2, we prove (for any fixed $A, B\in\mathbb{R}_+^{n\times n}$) that the next relation holds:

$$\rho(A+B)<1 \;\Rightarrow\; \rho(A+\nu B)<1 \quad \forall \nu\in\mathbb{D}. \tag{A.2}$$

To this end, we first prove

$$\rho(A+B)<1 \;\Rightarrow\; \rho(A+\nu B)<1 \quad \forall \nu\in\partial\mathbb{D}. \tag{A.3}$$

From $\rho(A+B)<1$ and $A+B\in\mathbb{R}_+^{n\times n}$, we see from [1] that there exists positive definite diagonal matrix P such that

$$\begin{bmatrix} -P & P(A+B) \\ (A+B)^T P & -P \end{bmatrix} \prec 0.$$

This reduces to

$$\begin{bmatrix} -I & (A_P+B_P) \\ (A_P+B_P)^T & -I \end{bmatrix} \prec 0,$$
$$A_P := P^{\frac{1}{2}} A P^{-\frac{1}{2}}, \quad B_P := P^{\frac{1}{2}} B P^{-\frac{1}{2}}.$$

Therefore $\|A_P+B_P\|<1$ holds for $A_P, B_P\in\mathbb{R}_+^{n\times n}$. This implies that $\|G\|_\infty<1$ holds for the discrete-time positive and stable system G given by

$$G(z) := \left[\begin{array}{c|c} 0 & I \\ \hline A_P & B_P \end{array}\right]$$

since $\|G\|_\infty = \|G(1)\| = \|A_P+B_P\|$ [11],[26]. From KYP lemma [27] for discrete-time LTI systems, we further obtain

$$\exists \Pi \succ 0 \text{ such that } \begin{bmatrix} -\Pi + A_P^T A_P & A_P^T B_P \\ B_P^T A_P & \Pi + B_P^T B_P - I \end{bmatrix} \prec 0.$$

It follows that

$$\begin{bmatrix} I \\ \nu I \end{bmatrix}^* \begin{bmatrix} -\Pi + A_P^T A_P & A_P^T B_P \\ B_P^T A_P & \Pi + B_P^T B_P - I \end{bmatrix} \begin{bmatrix} I \\ \nu I \end{bmatrix} \prec 0 \quad \forall \nu\in\partial\mathbb{D}$$

$$\Leftrightarrow (A_P+\nu B_P)^*(A_P+\nu B_P) \prec I \quad \forall \nu\in\partial\mathbb{D}$$

$$\Leftrightarrow \|A_P+\nu B_P\|<1 \quad \forall \nu\in\partial\mathbb{D}$$

$$\Leftrightarrow \begin{bmatrix} -P & P(A+\nu B) \\ (A+\nu B)^* P & -P \end{bmatrix} \prec 0 \quad \forall \nu\in\partial\mathbb{D}$$

This clearly shows $\rho(A+\nu B)<1$ ($\forall \nu\in\partial\mathbb{D}$) and hence (A. 3) has been proved.

Next we move onto the final stage of the proof. Note that (A. 3) (for any $A, B\in\mathbb{R}_+^{n\times n}$) implies

$$\rho(A+B)\geq\rho(A+\nu B) \quad \forall \nu\in\partial\mathbb{D}.$$

This further implies

$$\rho(A+rB)\geq\rho(A+\nu B) \quad \forall \nu\in\partial\mathbb{D}_r,$$
$$\mathbb{D}_r := \{\nu\in\mathbb{C}:\ |\nu|\leq r\}, \quad \partial\mathbb{D}_r := \{\nu\in\mathbb{C}:\ |\nu|=r\},$$

Moreover, from [Theorem 8.1.18 of [4]], we have

$$\rho(A+B)\geq\rho(A+rB) \quad \forall r\in[0,1].$$

To summarize, we arrive at

$$\rho(A+B)\geq\rho(A+\nu B) \quad \forall \nu\in\partial\mathbb{D}_r,\ \forall r\in[0,1]$$

and hence

$$\rho(A+B)\geq\rho(A+\nu B) \quad \forall \nu\in\mathbb{D}.$$

This completes the proof. ■

Yoshio Ebihara (Member)

He received the B.E., M.E. and D.E. degrees in electrical engineering from Kyoto University, Kyoto, Japan, in 1997, 1999 and 2002, respectively. Since 2002, he has been with the Department of Electrical Engineering, Kyoto University, where he is an Associate Professor since 2010. His research interests include convex optimization in control and positive system analysis and synthesis. Currently, he is an Associate Editor of IEEE Transactions on Control Systems Technology, Automatica, and a board member of IET Control Theory and Applications. He is also the chair of IEEE CSS Technical Committee on Systems with Uncertainty.

Dimitri Peaucelle

He received his Ph.D. degree in 2000 from Toulouse University. He is a full-time researcher at the French National Center for Scientific Research (CNRS), working at LAAS in Toulouse. His research interests are in robust control, and extend to convex optimization over linear matrix inequalities (LMIs), periodic systems, time-delay systems and direct adaptive control. He is also involved in computer-aided control design activities and leads a project for control-oriented software development. He is the main contributor to the Robust Multiobjective Control (RoMulOC) Toolbox.

Denis Arzelier

He received the Diplôme d'Ingenieur (Engineer's Degree) from the Ecole Nationale Supérieure des Arts et Métiers, (ENSAM), Paris, 1989, the Diplôme d'Etudes Approfondies (Master's Degree) with specialization in control from the Ecole Centrale, Lille, France, in June 1990. From October 1990 to June 1992 he was a Ph.D. student at the Laboratoire d'Analyse et d'Architecture des Systemes of the Centre National de la Recherche Scientifique (LAAS-CNRS), Toulouse, France. He received the Ph.D. degree from INSA, Toulouse, France, in June 1992. Since October 1993 he is holding a research position at LAAS-CNRS, Toulouse, France. His research interests include robust control, convex optimization, and optimal control for aerospace.